



Eckert, R., Freyland, J. M., Gersen, H., Heinzelmann, H., Schurmann, G., Noell, W., ... de Rooij, N. F. (2000). Near-field fluorescence imaging with 32 nm resolution based on microfabricated cantilevered probes. *Applied Physics Letters*, 77(23), 3695 - 3697. 10.1063/1.1330571

Link to published version (if available):
[10.1063/1.1330571](https://doi.org/10.1063/1.1330571)

[Link to publication record in Explore Bristol Research](#)
PDF-document

University of Bristol - Explore Bristol Research

General rights

This document is made available in accordance with publisher policies. Please cite only the published version using the reference above. Full terms of use are available:
<http://www.bristol.ac.uk/pure/about/ebr-terms.html>

Take down policy

Explore Bristol Research is a digital archive and the intention is that deposited content should not be removed. However, if you believe that this version of the work breaches copyright law please contact open-access@bristol.ac.uk and include the following information in your message:

- Your contact details
- Bibliographic details for the item, including a URL
- An outline of the nature of the complaint

On receipt of your message the Open Access Team will immediately investigate your claim, make an initial judgement of the validity of the claim and, where appropriate, withdraw the item in question from public view.

Near-field fluorescence imaging with 32 nm resolution based on microfabricated cantilevered probes

Rolf Eckert, J. Moritz Freyland, Henkjan Gersen, Harry Heinzlmann, Gregor Schürmann et al.

Citation: *Appl. Phys. Lett.* **77**, 3695 (2000); doi: 10.1063/1.1330571

View online: <http://dx.doi.org/10.1063/1.1330571>

View Table of Contents: <http://apl.aip.org/resource/1/APPLAB/v77/i23>

Published by the [American Institute of Physics](http://www.aip.org).

Related Articles

Instrumentation for dual-probe scanning near-field optical microscopy
Rev. Sci. Instrum. **83**, 083709 (2012)

Quantitative coherent scattering spectra in apertureless terahertz pulse near-field microscopes
Appl. Phys. Lett. **101**, 011109 (2012)

Pump-probe scanning near field optical microscopy: Sub-wavelength resolution chemical imaging and ultrafast local dynamics
Appl. Phys. Lett. **100**, 153103 (2012)

Background-free imaging of plasmonic structures with cross-polarized apertureless scanning near-field optical microscopy
Rev. Sci. Instrum. **83**, 033704 (2012)

Scanning absorption nanoscopy with supercontinuum light sources based on photonic crystal fiber
Rev. Sci. Instrum. **82**, 123102 (2011)

Additional information on *Appl. Phys. Lett.*

Journal Homepage: <http://apl.aip.org/>

Journal Information: http://apl.aip.org/about/about_the_journal

Top downloads: http://apl.aip.org/features/most_downloaded

Information for Authors: <http://apl.aip.org/authors>

ADVERTISEMENT



HAVE YOU HEARD?

Employers hiring scientists
and engineers trust
physicstodayJOBS



<http://careers.physicstoday.org/post.cfm>

Near-field fluorescence imaging with 32 nm resolution based on microfabricated cantilevered probes

Rolf Eckert,^{a)} J. Moritz Freyland, Henkjan Gersen,^{b)} and Harry Heinzlmann^{c)}
Centre Suisse d'Electronique et de Microtechnique CSEM S.A., Rue Jaquet-Droz 1, 2007 Neuchâtel, Switzerland

Gregor Schürmann, Wilfried Noell, Urs Stauer, and Nico F. de Rooij
Institut de Microtechnique, Université de Neuchâtel, Rue Jaquet-Droz 1, 2007 Neuchâtel, Switzerland

(Received 1 August 2000; accepted for publication 6 October 2000)

High-resolution near-field optical imaging with microfabricated probes is demonstrated. The probes are made from *solid quartz tips* fabricated at the end of silicon cantilevers and covered with a 60-nm-thick aluminum film. Transmission electron micrographs indicate a continuous aluminum layer at the tip apex. A specially designed instrument combines the advantages of near-field optical and beam-deflection force microscopy. Near-field optical data of latex bead projection patterns in transmission and of single fluorophores have been obtained in constant-height imaging mode. An artifact-free optical resolution of 31.7 ± 3.6 nm has been deduced from full width at half maximum values of single molecule images. © 2000 American Institute of Physics. [S0003-6951(00)05449-8]

Scanning near-field optical microscopy (SNOM) is a promising tool to meet current and future demands for high-resolution optical characterization. Despite some spectacular demonstrations of this technique,¹ its difficulty of operation and the often ambiguous interpretation of results have so far hindered its broad application.

In a common SNOM scheme, a subwavelength sized aperture probe is scanned over the surface at close distance. Both the properties of the probe and the ability to keep the probe-sample gap constant determine the quality of the image obtained.

Most of today's probes used with this SNOM scheme consist of a tapered optical fiber that is metal coated so that a small aperture is formed at the tip apex. These probes typically suffer from irregular aperture shapes, which degrade the emission characteristics, and from small taper angles leading to long damping regions and therefore low transmissivities. They are generally irreproducible and expensive since they are produced on a piece-by-piece basis. The high stiffness of the fiber perpendicular to the surface requires a feedback relying on the damping of a lateral oscillation of the fiber.² The physics of this "shear-force" interaction is poorly understood compared to that of the force interaction of atomic force microscopy (AFM), and its application to heterogeneous or soft samples is difficult and often subject to artifacts.

In this letter, we present the development of cantilevered near-field optical probes, which avoid most of the difficulties described earlier. The fabrication process based on microfabrication is inherently reproducible and highly parallel, i.e.,

inexpensive. The probe tips are mounted onto cantilevers and therefore allow all imaging modes of force microscopy. The most significant difference to similar work published before³⁻⁶ is that the tips are made of solid quartz (index of refraction 1.51). This reduces the cutoff radius for non-dissipative light propagation resulting in higher transmissivities and allows the manufacturing of tips with various shapes and heights of several tens of micrometers. High resolution imaging in transmission and using fluorescent contrast is demonstrated.

The microfabricated probes (Fig. 1) are rectangular-shaped silicon levers with aluminum coated solid quartz (fused silica) tips.⁷ The spring constants of the cantilevers were calculated to be 1 and 7 N/m, respectively. Due to the high stiffness of the cantilevers we did not observe snap-in events while approaching the surface and therefore scanning at constant height was feasible. For light coupling, windows were etched into the levers at the location of the tips. The tip structuring process follows an established procedure for producing sharp quartz tips with smooth surfaces.⁸ For this work, four-sided pyramidal or conical tips were employed with heights of 25 μm . Previously a process based on reactive ion etching was utilized to form a physical aperture at the tip apex.⁹ For the probes used in the experiments shown

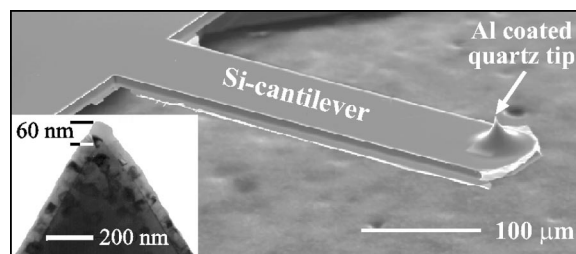


FIG. 1. Scanning electron microscopy image of a cantilevered microfabricated optical near-field probe with a cone-shaped quartz tip. Inset: TEM image of a 25 μm high quartz tip before use. The tip is completely covered with a 60-nm-thick aluminum layer.

^{a)}Also at: Institute of Physics, University of Basel, Klingelbergstr. 82, 4056 Basel, Switzerland; electronic mail: rolf.eckert@csem.ch

^{b)}Permanent address: Faculty of Applied Physics & MESA⁺ Research Institute, University of Twente, P.O. Box 217, 7500 AE Enschede, The Netherlands.

^{c)}Electronic mail: harry.heinzlmann@csem.ch

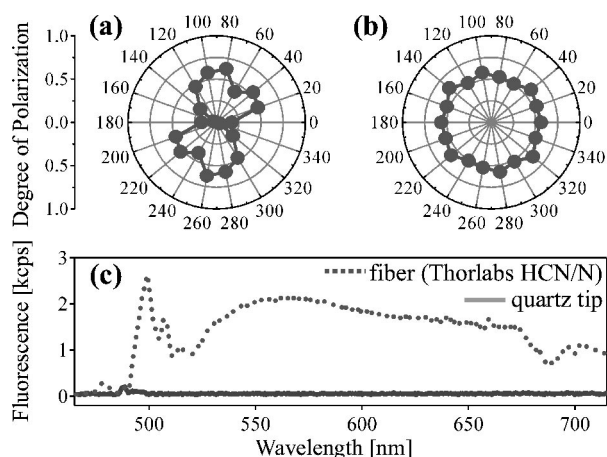


FIG. 2. Degree of polarization calculated as $(I_{\max} - I_{\min}) / (I_{\max} + I_{\min})$ for varying angles of linear polarized light coupled into the probe for (a) a four-sided pyramidal and (b) a conical tip. (c) Spectra of the autofluorescence of a microfabricated probe with solid quartz tip (solid line) and for comparison of a conventional 20 cm long optical fiber probe (dashed line).

here, this process was not performed. Transmission electron microscopy (TEM) indicates that an intact 60-nm-thick aluminum film is present at the tip apex (Fig. 1 inset). As presented later, these probes show far-field light transmission and allow near-field imaging below the diffraction limit.

The suitability of the probes for polarization and fluorescence measurements was evaluated by measuring their polarization and autofluorescence properties. The degree of polarization (DOP) of light transmitted through the aperture is shown in Fig. 2(a) for a four-sided pyramidal and in Fig. 2(b) for a conical tip. For both shapes the maximum value of the DOP is ~ 0.6 . For polarization measurements the conical geometry is more suitable because of its constant DOP for all directions compared to the orientation-sensitive DOP of the four-sided pyramidal tip.¹⁰ Figure 2(c) shows the autofluorescence spectra of a microfabricated probe (solid line) and of a conventional 20 cm long tapered optical fiber probe (dashed line). The advantage of the short transmission path length through the probe is clearly visible. The microfabricated probe with a short quartz tip contributes only minimally to the fluorescence background, whereas the spectrum of the optical fiber probe exhibits a high autofluorescence and Raman scattering of considerable strength.

A dedicated microscope was developed in order to perform cantilever-based SNOM (Fig. 3). The cantilever is mounted at a 15° angle to the sample in a home-built tripod microscope head, which is placed on top of an inverted optical microscope (Axiovert 135, Zeiss). Its deflection is monitored by an optical beam deflection scheme.¹¹ The sample is scanned in x - y direction by a closed-loop piezoelectric scanner and moved in the z direction by three coupled piezoelectric actuators. The feedback (670 nm) and the excitation light (488 nm) beam are brought together by a non-polarizing beamsplitter and focused onto the cantilever by the same lens. The transmitted excitation and the fluorescence light are collected by a microscope objective ($100\times$, numerical aperture=1.25), separated by a dichroic mirror and coupled into multimode fibers (core diameter $62.5 \mu\text{m}$) serving as spatial filters in the confocal arrangement. Additional filters in the fluorescence detection path reject residual

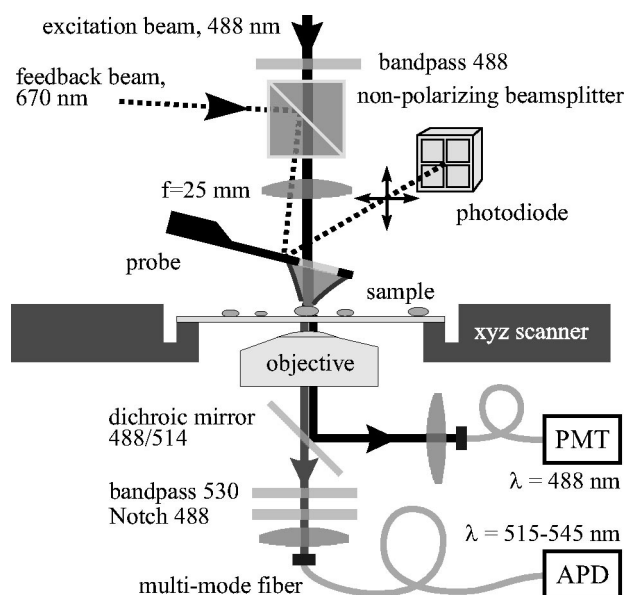


FIG. 3. Schematics of the experimental SNOM setup.

excitation and stray light from the feedback beam. A photomultiplier tube detects the transmitted excitation light and a single photon counting avalanche photodiode the fluorescence signal. Scanning and data acquisition are controlled by commercial scan electronics (STM 1000, RHK).

A latex bead projection pattern was imaged to determine the optical resolution achievable with the probes. It is produced by evaporating a 35-nm-thick aluminum film onto a hexagonal closed-packed monolayer of 220 nm diameter latex spheres. The beads are then washed away, leaving behind a regular array of metal islands on the glass substrate. We performed constant-height scans by pulling the tip out of the active feedback range.

The optical image of the transmitted light (Fig. 4) clearly reveals the hexagonal arrangement of the metal islands as dark spots along with some lattice defects. Assuming that the islands have perfectly steep edges, one can get an estimate of the optical resolution from the width of the measured edges. This would suggest an optical resolution of around 25 nm. However, as became evident after the experiment, the simultaneously acquired bending and friction signals indicate a residual force interaction between tip and sample. Since we

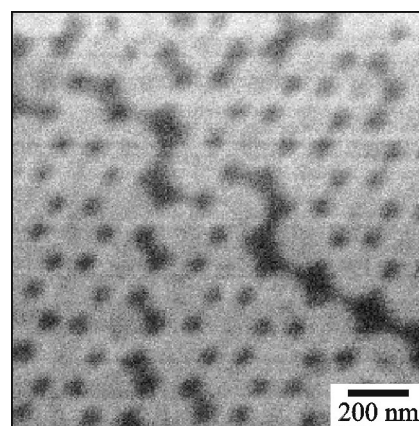


FIG. 4. Near-field optical image (512×512 pixels) of the light transmission through a 220 nm latex bead projection pattern.

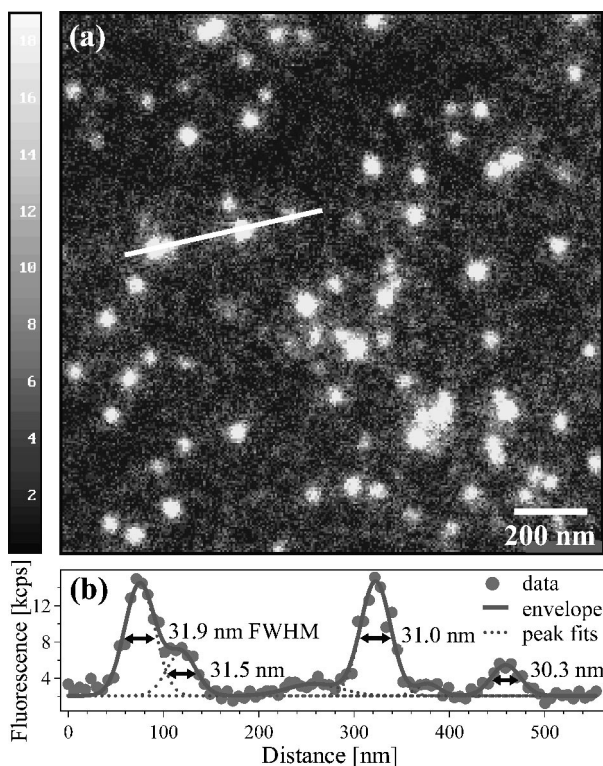


FIG. 5. (a) Near-field fluorescence image (256×256 pixels, 4 ms bintime) of fluorescently labeled proteins acquired in constant-height mode. (b) Cross section taken along the white line. The data (dots) can be reproduced by a multiplex fit (solid line). The optical resolution given by the FWHM value of the peaks (dashed lines) is better than 32 nm. The average FWHM of 47 molecules in the image yields an optical resolution of 31.7 ± 3.6 nm.

can quantify neither the crosstalk between topographical features and the optical signal¹² nor the influence of the cantilever's bending on the light coupling into the tip, the value for the optical resolution given earlier might be influenced by topography artifacts.

A better measure of the optical resolution is the image of a point-like light source such as individual fluorescently labeled biomolecules.¹³ To this purpose goat anti-rat antigens were labeled with AlexaFluor 488 (Molecular Probes) with a binding ratio of 1.5 fluorophores per protein and diluted in buffer to a concentration of 10^{-6} M. Then the proteins were deposited by spin coating on a glass cover slip, which was previously cleaned by dipping it shortly into 2% hydrofluoric acid and rinsing it thoroughly in high-purity water. According to previous experiments a surface density of roughly 10 proteins per $1 \mu\text{m}^2$ was expected. The sample was scanned in constant-height mode with a gap width of around 10 nm between tip and surface.

The near-field fluorescence image [Fig. 5(a)] shows approximately 85 peaks attributed to individual proteins with 1 or 2 attached fluorophores, respectively. The simultaneously acquired topography, bending, and friction signals (not shown) exhibit no variations over the whole scan confirming true constant-height operation. The maximum fluorescence

count rate is ~ 16 kcps with an excellent signal-to-noise ratio. A measure of the lateral optical resolution is the full width at half maximum (FWHM) value of the fluorescence peaks. Cross sections along the 47 brightest molecules were taken and fitted with a Gaussian distribution. An example is shown in Fig. 5(b). The four individual peaks can be reproduced by a multiplex fit revealing a resolution better than 32 nm. The average of the FWHM values for all 47 molecules results in an optical resolution of 31.7 ± 3.6 nm. It is worth noting the small variation of the averaged FWHM value, which indicates that the probe did not alter during the scan.

In conclusion, we have demonstrated near-field optical imaging with a true optical resolution of 32 nm utilizing microfabricated cantilevered probes with solid quartz tips. TEM images indicate a closed aluminum layer at the tip apex. Optical characterization of the probes shows good polarization characteristics and low autofluorescence making them eminently suitable for fluorescent imaging. At this point, the explanation of the experimental findings is not clear. While the far-field measurements can be understood in terms of residual light transmission through a finite metal film, this cannot account for the high-resolution near-field data. These could be explained by coupling to modes propagating at the outside surface of the metal coating, in combination with field localization at the metal tip. A discussion will be given in a forthcoming publication.⁷ The accidental formation of a small aperture during tip approach seems unlikely.

We feel confident that the development of cantilevered microfabricated probes opens the door to high-resolution near-field optical imaging of delicate samples in fluid environments.

This work was partially funded by the Swiss Priority Program MINAST.

¹ *Proceedings of the 5th International Conference on Near-Field Optics and Related Techniques (NFO-5)*, Shirahama, Japan, 1998, edited by T. Wilson (Blackwell Science Ltd, Oxford, 1999).

² E. Betzig, P. L. Finn, and J. S. Weiner, *Appl. Phys. Lett.* **60**, 2484 (1992).

³ F. Baida, D. Courjon, and G. Tribillon, *NATO ASI Ser. E* **242**, 71 (1993).

⁴ H. Zhou, A. Midha, G. Mills, S. Thoms, S. K. Murad, and J. M. Weaver, *J. Vac. Sci. Technol. B* **16**, 54 (1998).

⁵ A. Vollkopf, O. Rudow, T. Leinhos, C. Mihalcea, and E. Oesterschulze, *J. Microsc.* **194**, 344 (1999).

⁶ W. Noell, M. Abraham, W. Ehrfeld, M. Lacher, and K. Mayr, *J. Micro-mech. Microeng.* **8**, 111 (1998).

⁷ G. Schürmann, W. Noell, U. Staufer, N. F. de Rooij, R. Eckert, J. M. Freyland, H. Gersen, and H. Heinzlmann (unpublished).

⁸ M.-A. Grétilat, F. Paoletti, P. Thiébaud, S. Roth, M. Koudelka-Hep, and N. F. de Rooij, *Sens. Actuators A* **60**, 219 (1997).

⁹ G. Schürmann, P. F. Indermühle, U. Staufer, and N. F. de Rooij, *Surf. Interface Anal.* **27**, 299 (1999).

¹⁰ T. Lacoste, T. Huser, R. Prioli, and H. Heinzlmann, *Ultramicroscopy* **71**, 333 (1998).

¹¹ G. Meyer and N. M. Amer, *Appl. Phys. Lett.* **53**, 1045 (1988).

¹² E. Betzig and J. K. Trautman, *Science* **257**, 189 (1992).

¹³ J. A. Veerman, M. F. Garcia-Parajo, L. Kuipers, and N. F. van Hulst, *J. Microsc.* **194**, 477 (1999).